Absorption of Fast Waves by Electrons on the DIII-D Tokamak

C. C. Petty, R. I. Pinsker, M. J. Mayberry,[a] M. Porkolab,[b] F. W. Baity,[c] P. T. Bonoli,[b] S. C. Chiu, J. C. M. de Haas,[d] R. H. Goulding,[c] D. J. Hoffman,[c] T. C. Luce, and R. Prater

General Atomics, P.O. Box 85608, San Diego, California 92186

(Received 13 February 1992)

Efficient direct heating of electrons by fast waves has been observed on the DIII-D tokamak. The measured fast-wave heating efficiency was independent of magnetic field, in contrast to the strong inverse magnetic field scaling predicted by the theory of single-pass damping, indicating multiple-pass absorption. The central heating of electrons by the fast waves had a strong dependence on the target electron temperature. *H*-mode plasmas were obtained with fast-wave heating alone for the first time in the direct electron heating regime.

PACS numbers: 52.50.Gj, 52.40.Db, 52.55.Fa

Research in magnetic confinement fusion is presently centered around the tokamak [1], a machine with closed magnetic geometry in which the plasma is confined by a combination of a large toroidal magnetic field imposed by external magnets and a smaller poloidal magnetic field generated by a toroidal plasma current. The plasma current is normally induced by transformer action, and therefore is transient. Auxiliary heating (that is, noninductive heating) may be used on tokamaks to increase the plasma temperature so that the thermonuclear fuel may ignite, as well as to drive the plasma current independently of the transformer and thus allow steady-state operation. One method of radio frequency (rf) heating which theoretically shows promise in achieving both the heating and current-drive goals is the direct absorption by electrons of the fast (magnetosonic) wave [2–4].

The fast wave is a compressional wave that propagates primarily perpendicular to the static magnetic field [5]. Ion cyclotron resonance heating (ICRH) by fast waves has previously been used to heat tokamak plasmas [6]; however, fast waves can also be absorbed directly by electrons when the resonance condition $\omega - k_{\parallel}v_{\parallel e} = 0$ is satisfied (ω is the frequency of the fast wave, $k_{\parallel}$ is the wave number parallel to the magnetic field, and $v_{\parallel e}$ is the electron velocity parallel to the magnetic field). The direct electron absorption of fast waves is due to electron Landau damping and transit-time magnetic pumping [7]. For a Maxwellian electron distribution, the *e*-folding damping length at low frequencies is given by [8]

$$\lambda_e^{-1} = k_{\perp Re}\frac{\sqrt{\pi}}{2}\beta_e\xi_e\exp(-\xi_e^2)\left[1+\frac{1}{\alpha^2}\right], \qquad (1)$$

where $k_{\perp Re} \approx \omega/v_A$, $v_A = c\,\Omega_i/\omega_{pi}$, $\beta_e = 2\mu_0 n_e T_e/B^2$, $\xi_e = \omega/k_{\parallel}v_{te}$, $v_{te} = (2T_e/m_e)^{1/2}$, and α is a complicated function with $\alpha^{-2} < 1$ for this experiment. The fast-wave absorption is maximized when $\xi_e = 1/\sqrt{2}$, and it decreases rapidly with increasing magnetic field since $\lambda_e^{-1} \propto B^{-3}$.

The fast-wave experiments reported in this Letter were aimed at characterizing the direct electron heating of fast waves in the ion cyclotron range of frequencies (ICRF) as ξ_e and B were varied. In general, fast-wave heating was found to be efficient on DIII-D as is evident from the nearly 100% absorption of the fast-wave energy by the plasma and the obtainment of *H*-mode plasmas. JET and JFT-2M have recently reported evidence of fast-wave damping on thermal electrons in the ICRF; however, only about 20% of the fast-wave power was directly absorbed by electrons [9,10]. For JET, the direct electron heating by fast waves was limited to first-pass absorption since a strong ion cyclotron resonance was present near the plasma center [9]. For JFT-2M, the direct electron heating was inefficient because the fast-wave parallel phase velocity was much larger than the electron thermal velocity ($\xi_e \gtrsim 1.7$) [10]. The DIII-D experiments reported in this Letter have neither of these limitations.

The fast-wave heating experiments on the DIII-D tokamak [11] were performed in double-null-divertor discharges using deuterium gas puffing. The fast waves were launched at 60 MHz using a phased array of four loop antennas. When the relative phase between the currents in the four straps is $(0,\pi,0,\pi)$, the launched parallel index of refraction is $|n_{\parallel}| \equiv |k_{\parallel}|c/\omega \approx 9$, which is optimal for direct electron absorption at electron temperatures near 3 keV after accounting for the upshift of the spectrum due to toroidal effects.

Efficient plasma heating was seen during fast-wave injection on DIII-D, as shown in Fig. 1. The toroidal magnetic field was 1.6 T which placed the second and third hydrogen cyclotron harmonics near the plasma edge ($\rho \approx 0.73$, where ρ is the normalized radius) on either side of the plasma center, thereby reducing the possibility of significant ion cyclotron absorption by the residual hydrogen in the deuterium discharge. During fast-wave heating the plasma stored energy increased as well as the central electron temperature determined from Thomson scattering. The Ohmic power decreased during fast-wave heating as a result of the electron heating.

Coating the antenna and nearby tokamak vessel wall surfaces with low-*Z* materials (such as boron or carbon) was found to be effective in reducing metal influx and radiated power [12]. Boronization was found to be the

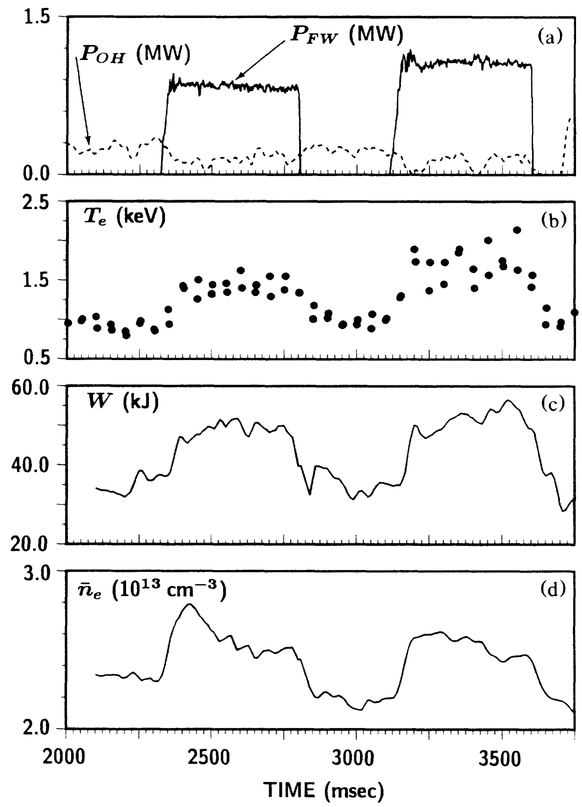

FIG. 1. Time history of (a) net fast-wave and Ohmic power, (b) central electron temperature, (c) plasma stored energy, and (d) line-averaged density. The coupled fast-wave power is 80% of the net power (I_p =300 kA, B_T =1.6 T, κ=1.4, deuterium discharge with ≈ 2% hydrogen fraction).

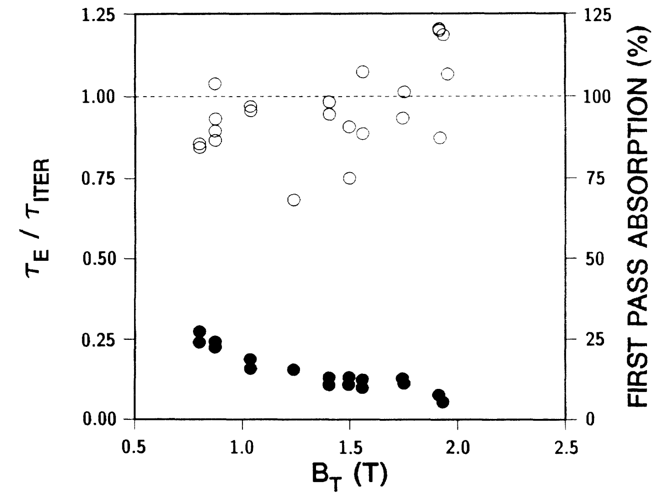

FIG. 2. Energy confinement time (open circles) normalized to the ITER-89 power-law scaling relation as a function of the toroidal magnetic field for high-aspect-ratio plasmas (R =1.86 m, a =0.48 m, I_p =300 kA, $\bar{n} \approx 2.5\times10^{19}$ m^{-3}, κ=1.4). Also shown is the calculated first-pass absorption (solid circles).

most effective wall conditioning technique, reducing the incremental radiated power fraction to $\Delta P_{rad}/P_{rf} \approx 0.3$, regardless of the antenna phasing. Boronization also reduced the plasma density increase which occurs during 60-MHz fast-wave injection.

The magnetic field scaling of Eq. (1) was investigated by scanning the toroidal magnetic field at constant plasma curent and density from 0.8 to 2.0 T. The plasma stored energy (W) at each magnetic field was determined from reconstruction of the plasma equilibrium using external magnetic measurements [13]. The stored energy determined in this manner agreed well with the diamagnetic and kinetic measurements of the plasma stored energy. In order to normalize out the weak magnetic field scaling of the energy confinement time ($\tau_E = W/P$, where P is the total Ohmic and injected rf power) present for any form of auxiliary heating, the experimentally measured τ_E is divided by the ITER-89 power-law scaling relation developed for the ITER design [14]:

$$\tau_E = 0.048 I^{0.85} R^{1.2} a^{0.3} \bar{n}^{0.1} B_T^{0.2} (A\kappa/P)^{0.5}, \qquad (2)$$

where τ_E is in sec, I is the plasma current in MA, R and a are the major and minor radii in m, $\bar{n}$ is the electron density in 10^{20} m^{-3}, B_T is the toroidal magnetic field in T, A is the atomic mass number, κ is the elongation, and P is the total power in MW. The ITER scaling relations agree with the measured energy confinement time for electron cyclotron resonance heated [15] (ECRH) as well as neutral beam injection (NBI) heated plasmas [14] on DIII-D. The plasma parameter values for Eq. (2) are taken during the steady-state portion of the rf pulse.

The normalized energy confinement time during fast-wave heating for a magnetic field scan was independent of B_T, as shown in Fig. 2 for high-aspect-ratio plasmas (similar results were obtained in full size discharges). Assuming that the ITER-89 power-law scaling relation [Eq. (2)] accurately predicts the actual energy confinement time, then the normalized energy confinement time represents the fraction of absorbed fast-wave power [i.e., $\eta = (W/P)/\tau_E^{ITER}$]. The first-pass absorption calculated from a slab model [4] is also shown in Fig. 2 for comparison. (The central electron temperature increased with B_T; however, this effect is included in the calculation of the first-pass absorption.) Although the calculated first-pass absorption decreased from 27% to 5% as the toroidal magnetic field was varied from 0.8 to 2.0 T, the absorbed power fraction was independent of B_T and had a value of $\eta = 0.96 \pm 0.13$. This estimate of the absorbed power fraction used the injected rf power in Eq. (2); if the absorbed rf power is used instead then η drops slightly to 0.94. Therefore the efficiency of direct electron heating by fast waves is nearly 100% even for discharges where the first-pass absorption is weak. This indicates either that multiple-pass absorption of the fast waves is occurring or that the damping is much stronger than Eq. (1) predicts.

Since there is a second-harmonic hydrogen resonance passing through the magnetic axis for $B_T = 2$ T, ion cyclotron absorption may compete with direct electron absorption at this toroidal field. However, since the hydrogen fraction is low ($\approx 2\%$ measured by edge spectroscopy), full wave code calculations show that the direct electron damping is typically 5 times stronger than the second-harmonic hydrogen damping under these conditions [16].

The direct electron heating by fast waves was found to be sensitive to the target electron temperature at a fixed magnetic field, in contrast to the absence of any observable magnetic field scaling of the fast-wave absorption. The Ohmic electron temperature was scanned by varying the electron density from 1.1×10^{19} to 1.9×10^{19} m^{-3}. The toroidal magnetic field was 1.4 T for this experiment, which placed the third-harmonic cyclotron resonance for hydrogen near the plasma center. As shown in Fig. 3, the electron heating effectiveness, defined as

$$\eta e = \Delta T_e(0)\bar{n}_e V / P_{\mathrm{FW}}, \qquad (3)$$

where V is the plasma volume, increased substantially as the target electron temperature increased above 1 keV. This temperature corresponds to a ratio of the (toroidally downshifted) wave parallel phase velocity to the electron thermal velocity of $\xi_e \approx 1.3$. It is not understood at this time why the fast-wave heating should depend upon ξ_e and not B_T.

Finally, for the first time in the direct electron heating regime, H-mode plasmas have been obtained with fast-wave heating alone (H-mode period $\gg$ energy confinement time), as shown in Fig. 4. The regime of "high" confinement was first achieved with NBI heating on ASDEX [17], but subsequently has been achieved during ICRH [18], ECRH [19], and even Ohmic heating [20]. Obtainment of the H mode in the direct electron absorption regime is strong evidence of efficient heating by the fast waves. For the H-mode plasma in Fig. 4, ion cyclotron damping of the fast wave was negligible since $\omega = 8\Omega_D$. The power threshold for H mode with fast-wave heating was somewhat lower than the power threshold for ECRH or NBI heating [21]. For this discharge the fast-wave power was very close to the threshold power, so the H mode was preceded by a relatively long L-mode period. Upon transition to the H mode, the divertor light dropped and signs of edge localized modes (ELMs) appeared. At the same time the electron density and stored energy began to increase, indicating an improved particle and energy confinement time. The plasma current profile also broadened, evidenced by the lower normalized internal inductance, as is characteristic of H modes. There was no significant impurity accumulation during the H-mode phase. The enhancement in energy confinement between L mode and H mode was 1.54 for this shot; at slightly higher fast-wave power the enhancement in confinement was 2.0. Quasi-steady-state ELM

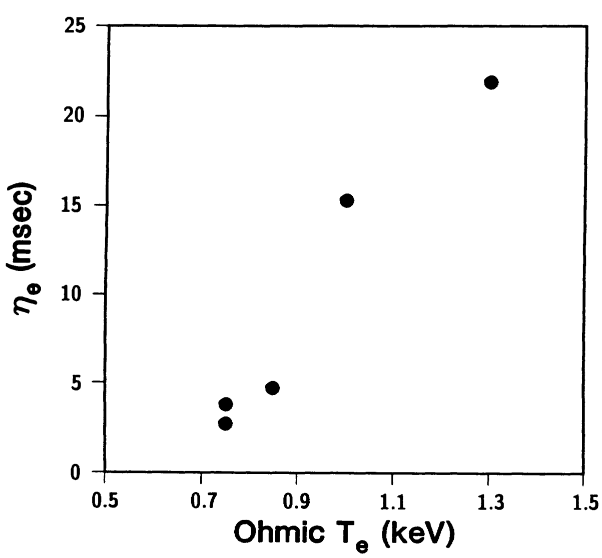

FIG. 3. Electron heating effectiveness as a function of the target electron temperature [$I_p = 510$ kA, $B_T = 1.4$ T, $\bar{n} = (1.1-1.9)\times10^{19}$ m^{-3}, $\kappa = 1.9$].

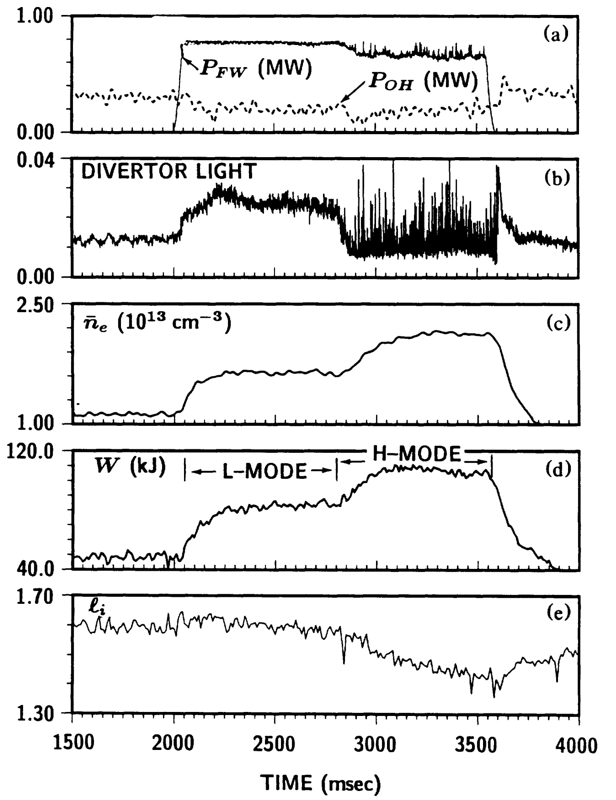

FIG. 4. Time history of (a) net fast-wave and Ohmic power, (b) divertor light, (c) line-averaged electron density, (d) plasma stored energy, and (e) normalized internal inductance. A transition from L-mode confinement to H-mode confinement occurs around 2850 msec, and the H mode continues until the fast-wave power is removed ($I_p = 510$ kA, $B_T = 1.0$ T, $\kappa = 1.9$).

H-mode periods as long as 1350 msec have been produced in similar discharges; the rf pulse length is presently limited by Joule heating of the uncooled antenna.

In summary, highly efficient direct electron heating with 60-MHz fast waves has been observed on the DIII-D tokamak. Nearly 100% absorption was measured for all magnetic fields, indicating that multiple-pass absorption was occurring. The electron heating effectiveness of the fast waves increased with increasing target electron temperature, and a threshold for good central electron heating of $\omega/k_{\parallel} \lesssim 1.3 v_{te}$ was observed. H-mode plasmas were obtained for the first time by fast-wave heating in the direct electron heating regime. The efficient direct electron heating observed on DIII-D points to an alternative method of plasma heating by fast waves which does not require a match between the applied frequency and the magnetic field.

The authors wish to thank T. H. Osborne and T. S. Taylor for their efforts in developing the high-aspect-ratio plasmas used in these experiments. This work was supported by the U.S. Department of Energy under Contracts No. DE-AC03-89ER51114, No. DE-AC05-84-OR21400, and No. DE-AC02-78ET51013.

[a]Present address: Stanford University, Stanford, CA.

[b]Present address: Massachusetts Institute of Technology, Cambridge, MA 02139.

[c]Present address: Oak Ridge National Laboratory, Oak Ridge, TN 37831.

[d]Also at Lawrence Livermore National Laboratory, Livermore, CA 94550.

[1] J. A. Wesson, *Tokamaks* (Clarendon, Oxford, 1987).

[2] N. J. Fisch and C. F. F. Karney, Phys. Fluids **24**, 27 (1981).

[3] R. W. Harvey, K. D. Marx, and M. G. McCoy, Nucl. Fusion **21**, 153 (1981).

[4] S. C. Chiu, V. S. Chan, R. W. Harvey, and M. Porkolab, Nucl. Fusion **29**, 2175 (1989).

[5] T. H. Stix, *The Theory of Plasma Waves* (McGraw-Hill, New York, 1962).

[6] D. G. Swanson, Phys. Fluids **28**, 2645 (1985).

[7] T. H. Stix, Nucl. Fusion **15**, 737 (1975).

[8] M. Porkolab, in *Radiofrequency Power in Plasmas,* Proceedings of the Ninth Topical Conference, Charleston, SC, 1991 (American Institute of Physics, New York, 1992), p. 197.

[9] L.-G. Eriksson and T. Hellsten, Nucl. Fusion **29**, 875 (1989).

[10] T. Yamamoto *et al.*, Phys. Rev. Lett. **63**, 1148 (1989).

[11] J. L. Luxon and L. G. Davis, Fusion Technol. **8**, 441 (1985).

[12] M. J. Mayberry *et al.*, in *Radiofrequency Power in Plasmas* (Ref. [8]), p. 276.

[13] L. L. Lao, H. St. John, R. D. Stambaugh, A. G. Kellman, and W. Pfeiffer, Nucl. Fusion **25**, 1611 (1985).

[14] ITER Team, "ITER Conceptual Design—Interim Report" (IAEA, Vienna, 1989).

[15] T. C. Luce *et al.*, in *Plasma Physics and Controlled Nuclear Fusion 1990*, Thirteenth Conference Proceedings, Washington, DC, 1990 (IAEA, Vienna, 1991), Vol. 1, p. 631.

[16] P. T. Bonoli and M. Porkolab, in *Radiofrequency Power in Plasmas* (Ref. [8]), p. 155.

[17] F. Wagner *et al.*, Phys. Rev. Lett. **49**, 1408 (1982).

[18] K. Steinmetz *et al.*, Phys. Rev. Lett. **58**, 124 (1987).

[19] John Lohr *et al.*, Phys. Rev. Lett. **60**, 2630 (1988).

[20] T. H. Osborne *et al.*, Nucl. Fusion **30**, 2023 (1990).

[21] K. H. Burrell *et al.*, *Plasma Physics and Controlled Nuclear Fusion Research 1988*, Twelfth Conference Proceedings, Nice, Italy, 1988 (IAEA, Vienna, 1989), Vol. 1, p. 193.